IET Power Electronics

Research Article

IET Journals
The Institution of Engineering and Technology

Simple control scheme for single-phase uninterruptible power supply inverters with Kalman filter-based estimation of the output voltage

ISSN 1755-4535
Received on 3rd December 2014
Revised on 19th March 2015
Accepted on 6th April 2015
doi: 10.1049/iet-pel.2014.0929
www.ietdl.org

Reza Razi, Mohammad Monfared ✉

Department of Electrical Engineering, Faculty of Engineering, Ferdowsi University of Mashhad, Mashhad, Iran
✉ *E-mail: m.monfared@um.ac.ir*

Abstract: The major drawback of most control methods for uninterruptible power supply (UPS) inverters is complexity. In this study, a simple voltage sensorless multi-loop control method is proposed for the single-phase UPS inverter and the parameters are designed systematically based on a frequency domain method. The suggested control scheme uses two nested simple proportional controllers instead of proportional–integral/resonant controllers to regulate the output voltage and produce active resonance damping. In addition, a feedforward compensation of the reference voltage is used to enhance the performance of the control system. The proposed controller does not need any reference frame transformation or integration/derivation of measured quantities in its structure. To reduce the cost and at the same time to improve the reliability of the converter system, the output voltage sensor is replaced by a simple estimation algorithm based on the digital Kalman filter. Experimental results with a 500 VA prototype, as well as simulation results validate the excellent performance of the suggested estimation and control scheme.

1 Introduction

Power electronic converters are employed in distributed generation (DG) systems to regulate the generated energy from small-scale sources such as photovoltaics, wind turbines, fuel cells and diesel generators. The DG unit in the stand-alone operation mode is the source of power, which is intended to supply high quality and reliable electricity to local or critical loads through a controlled voltage source inverter, usually called the uninterruptible power supply (UPS) inverter [1]. The UPS inverter should be able to support the local network or critical load with the appropriate voltage and frequency from the DC input. Many control methods for UPS inverters are available in the literature, including [2–4]: (i) model-based instantaneous feedback controllers, such as multi-loop controllers [5–7], (ii) repetitive controllers [8–12] and (iii) non-linear controllers [13–15].

The repetitive control is based on the internal model principle and in particular is used in dealing with periodic signals. This method has some drawbacks such as slow dynamics, large memory requirement and poor performance in the presence of non-periodic disturbances.

Although the non-linear controllers have some good features such as excellent dynamic performance, but these techniques also suffer from some limitations, such as steady-state errors, complexity and sensitivity to parameter variations. It is worth mentioning that some papers propose a combination of available methods to achieve a better performance [16].

A UPS inverter is usually connected to the AC load via an LC smoothing filter, as evident from Fig. 1. This filter is required for attenuating the switching noises. However, harmonic components generated by the inverter can cause resonance oscillations with an ideally lossless LC filter. In general, two techniques are available to tackle this problem, including passive and active damping techniques. Passive damping method employs a physical resistor in the filter circuit. In another method, the active damping uses an additional loop that plays the role of the virtual resistance for damping the resonance oscillations. More control flexibility and higher efficiency because of avoiding the losses are characterised as the main advantages of the multi-loop controllers.

The major drawbacks associated with the multi-loop control schemes are complexity of design of parameters of outer and inner control loops and several sensors necessary for measuring feedback variables in the nested control loops. Therefore it is favourable to use simple proportional controllers instead of proportional–integral (PI) or proportional–resonant (PR) regulators in both control loops and reduce the number of sensors, if possible.

Consequently, several estimation methods have been proposed to replace some measurement sensors with software algorithms. These algorithms use the system parameters and other measured quantities as the inputs to estimate the instantaneous values of desired quantities [7, 17–20]. Adaptive control is used to estimate the output voltage for sensorless operation in [7], which enhances the system robustness and performance. In [17], a novel adaptive estimation unit, with low computational burden, is designed to estimate the interfacing parameters and grid voltages simultaneously. In [18], the controller uses the model of the system to predict, on each sampling interval, the behaviour of the output voltage for each possible switching state, and an observer is used for load current estimation. A digital adaptive controller, based on the generalised minimum variance control approach, for high-performance single-phase inverters is proposed in [19]. Moreover in [20], the grid voltage sensors are replaced by a voltage estimation scheme based on the Newton–Raphson algorithm.

In this paper, a simple voltage sensorless multi-loop control method is proposed and designed for single-phase UPS inverters. The suggested multi-loop control scheme uses two variables as feedback signals, which regulates them with simple proportional controllers. The outer loop tracks the voltage reference signal and the inner loop actively damps the possible resonances because of the LC filter by regulating the capacitor current. For this purpose, the capacitor current is obtained indirectly from the measured converter and load currents. The load voltage is estimated by the Kalman filter algorithm, which is described in details in Section 4. Moreover, a feedforward compensation of the reference voltage is used, which improves the performance of the controller. The parameters of the controller are designed step-by-step based on the

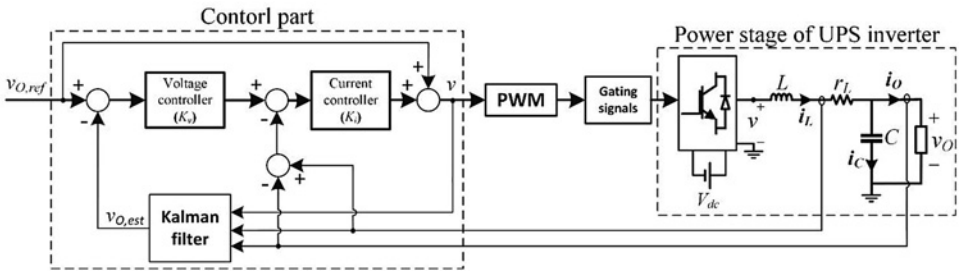

Fig. 1 *Power stage of UPS inverter with suggested control scheme*

decided bandwidths for the inner and outer control loops. Finally, the performance of the proposed control method is confirmed through extensive simulations and experiments.

2 System description

The schematic diagram of the power stage of the single-phase UPS inverter is shown in Fig. 1. The circuit parameters are summarised in Table 1. The voltage at the DC bus is assumed to be constant by using enough capacitance and also the equivalent series resistance of the filter capacitor is ignored.

On the basis of Fig. 1, mathematical model of the single-phase UPS inverter can be derived as

$$v = r_{\mathrm{L}} i_{\mathrm{L}} + L\frac{\mathrm{d}i_{\mathrm{L}}}{\mathrm{d}t} + v_{\mathrm{O}} \tag{1}$$

$$i_{\mathrm{L}} = i_{\mathrm{O}} + C\frac{\mathrm{d}v_{\mathrm{O}}}{\mathrm{d}t} \tag{2}$$

where v, v_{O}, i_{L} and i_{O} are the output voltage of the inverter, the load voltage, the filter (converter) current and load current, respectively. On the basis of (1) and (2) the model of the UPS inverter in the s-domain can be obtained as shown in Fig. 2.

3 Control strategy

3.1 Proposed control structure

The multi-loop control method of the UPS inverter includes the inner and outer feedback loops for current and voltage control, respectively. The outer loop is responsible for tracking the output voltage, whereas the inner loop provides active damping, stability over a wide range and fast dynamic for disturbances. Previous reported multi-loop control schemes for UPS inverters adopted PI or PR controllers in outer feedback loop and used filter inductor current, filter capacitor current and other different combinations of currents, as the inner loop control variable [21–29].

The proposed multi-loop control scheme, illustrated in Fig. 1, uses the simple proportional gains (K_i and K_v) as the current and voltage controllers and uses the filter capacitor current as the inner loop control variable. It is proved that the capacitor current feedback has better disturbance rejection capability than the inductor current feedback [1, 22]. Moreover, a reference voltage feedforward is added to reduce the control effort and improve the system robustness. With this scheme, the system analysis and controller design are significantly simplified because of the simple proportional controllers, and at the same time, avoiding the problem of phase delay at the fundamental frequency, associated to the PI and PR controllers.

For further hardware simplification, it will be shown in the next sections that the output voltage sensor can be eliminated by using an appropriate voltage estimator.

Table 1 System parameters

Parameter	Description	Value
f_s	sampling/switching frequency	20 kHz
f	fundamental frequency	50 Hz
V_{dc}	DC-link voltage	150 V
V_o	output voltage (root mean square)	70 V
C	filter capacitance	25 μF
L	filter inductance	3.7 mH
r_L	filter resistance	0.2 Ω
S	nominal power	500 VA

3.2 Design of the proposed controller parameters

3.2.1 Inner current control loop: In this paper, the proportional gains are chosen according to the required bandwidth of the control loops.

The UPS inverter with the inner control loop and the voltage feedforward is shown in Fig. 3. The closed-loop transfer function of the considered model is

$$G_i(s) = \frac{i_C}{i_{C,\mathrm{ref}}} = \frac{ZCK_iK_{\mathrm{PWM}}s}{ZCLs^2 + (ZC(r_{\mathrm{L}} + K_iK_{\mathrm{PWM}}) + L)s + Z - ZK_{\mathrm{PWM}} + r_{\mathrm{L}}} \tag{3}$$

It is demonstrated in [1] that the lowest control bandwidth for the inner loop is expected at the nominal load. Although conservative, the parameter of the inner control loop should be tuned under nominal loading conditions. The pulse width modulation (PWM) modulator is considered as a unity gain ($K_{\mathrm{PWM}} = 1$).

With considering the above assumptions, (3) can be simplified as follows

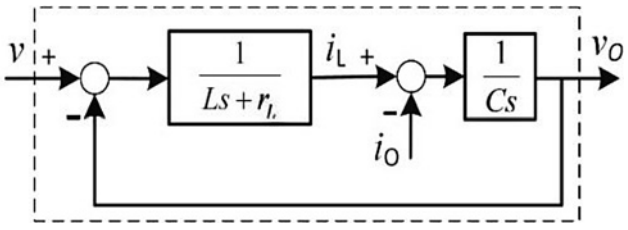

Fig. 2 *Block diagram of UPS inverter with LC filter*

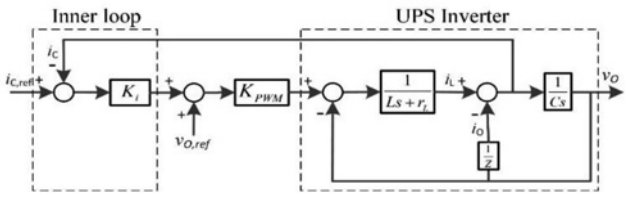

Fig. 3 *Inner current control loop*

IET Power Electron., 2015, Vol. 8, Iss. 9, pp. 1817–1824

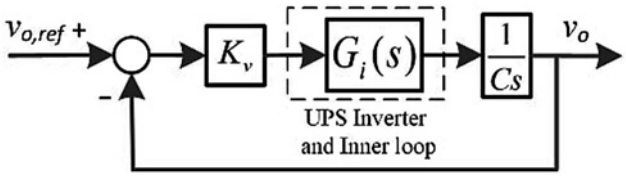

Fig. 4 *Simplified block diagram of the proposed control system*

$$G_i(s) = \frac{i_C}{i_{C,\text{ref}}} = \frac{Z_{\min} C K_i s}{Z_{\min} C L s^2 + (Z_{\min} C(r_L + K_i) + L)s + r_L} \quad (4)$$

In practice, the bandwidth of the inner control loop is considered enough lower than the switching frequency, because with high bandwidth, more noise could be coupled into the feedback loop. So here, the inner loop bandwidth is chosen as one-tenth of the switching frequency (f_s), that is

$$\omega_{bi} = 2\pi(0.1 \times f_s) = 2\pi(0.1 \times 20\,\text{kHz}) \simeq 12.5\,k\text{rad}/s \quad (5)$$

As a result, by solving $|G_i(j\omega_{bi})|^2 = 1/2$, the K_i is calculated to be about 66.

3.2.2 Outer voltage control loop: In the next step, the proportional controller of the outer control loop must be adjusted. The choice of the outer control loop gain (K_v) is a compromise between the bandwidth and stability of the outer control loop. The simplified block diagram of the proposed system is shown in Fig. 4, in which the inverter with the inner control loop is replaced by $G_i(s)$ from (4).

It should be noted that the phase margin (PM) may slightly change depending on the loading conditions (represented by the value of Z). The outer loop controller is tuned under the light load condition (Z tends to ∞). This assumption simplifies the analysis of the system and at the same time ensures the stability overall operating conditions [1]. The transfer function of the closed-loop system, with this assumption, can be written as

$$G(s) = \frac{v_o}{v_{o,\text{ref}}} = \frac{K_v K_i}{LCs^2 + C(r_L + K_i)s + K_v K_i} \quad (6)$$

The voltage control bandwidth must be decided according to a trade-off between the expected transient response and the disturbance rejection requirement. To obtain a fast transient response without scarifying the switching noise rejection, a bandwidth in the range of 20 times the fundamental frequency and one-tenth the switching frequency is a good compromise. In this paper, the outer loop bandwidth is chosen to be 1.5 kHz, which is in the middle of that range. By solving $|G(j\omega_{bv})|^2 = 1/2$ at $\omega_{bv} = 2\pi \times 1.5$ kHz ≈ 9.42 krad/s, the K_v is calculated to be about 0.18.

To examine the stability margin of the system, the bode plot of the open-loop transfer function is plotted in Fig. 5, which indicates that the PM is 69.4°. This value for the PM is enough for power electronic applications.

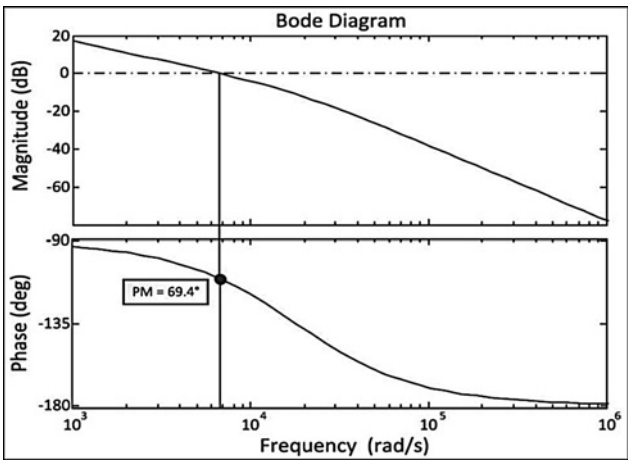

Fig. 5 *Open-loop bode plot of the voltage control loop*

4 Output voltage estimation with Kalman filter

In this paper, the output voltage is estimated by adopting the linear Kalman filter algorithm to our problem. For this purpose, a discrete-time state-space model of the system under study is needed. It should be noted that (1) characterises the inductance dynamics and (2) characterises the capacitor dynamics, while the load is assumed as a disturbance input to the converter system. These equations can be rewritten as a state-space equation as

$$\begin{bmatrix} \dot{i}_L \\ \dot{v}_O \end{bmatrix} = \begin{bmatrix} -\frac{r_L}{L} & -\frac{1}{L} \\ \frac{1}{C} & 0 \end{bmatrix} \begin{bmatrix} i_L \\ v_O \end{bmatrix} + \begin{bmatrix} \frac{1}{L} & 0 \\ 0 & -\frac{1}{C} \end{bmatrix} \begin{bmatrix} v \\ i_O \end{bmatrix} \quad (7)$$

This equation can be rewritten in the discrete form, assuming a sampling time T_s, as

$$\underbrace{\begin{bmatrix} i_L(k+1) \\ v_O(k+1) \end{bmatrix}}_{x(k+1)} = A_d \underbrace{\begin{bmatrix} i_L(k) \\ v_O(k) \end{bmatrix}}_{x(k)} + B_d \underbrace{\begin{bmatrix} v(k) \\ i_O(k) \end{bmatrix}}_{u(k)} \quad (8)$$

$$z(k) = Hx(k)$$

where

$$A_d = \begin{bmatrix} 1 - \frac{r_L T_s}{L} & -\frac{T_s}{L} \\ \frac{T_s}{C} & 1 \end{bmatrix}$$

and

$$B_d = \begin{bmatrix} \frac{T_s}{L} & 0 \\ 0 & -\frac{T_s}{C} \end{bmatrix}$$

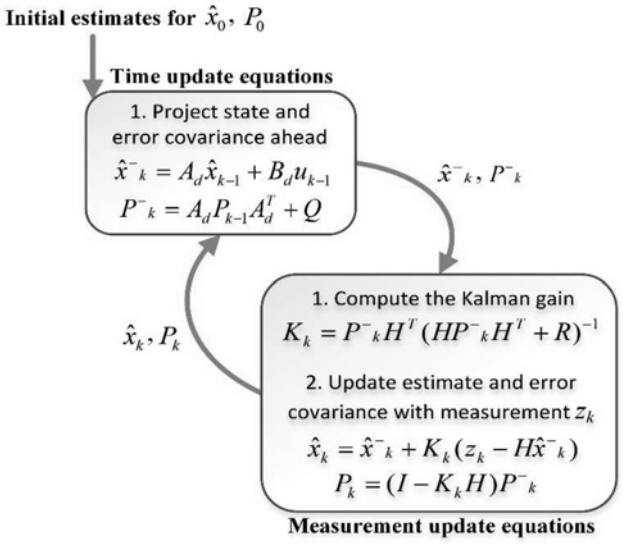

Fig. 6 *Kalman filter algorithm [31]*

This model is considered for the estimation algorithm. The measured filter inductor current is used to correct the estimates, therefore, $H = [1, 0]$ and

$$z(k) = i_L(k) \tag{9}$$

The Kalman algorithm for this system, as shown in Fig. 6, is composed of two sets of simple equations: time update and measurement update equations [30, 31]. The time update equation predicts the states and error covariance matrix one sample in advance to obtain the 'a priori' estimate for the next time step. Then the measurement update equation gives an improved 'posteriori' estimate by correcting the predictions through a feedback from actual measurement, here the filter inductor current. In the first step to estimate, initial values for state variables ($\hat{\boldsymbol{x}}_0$) and error covariance ($\boldsymbol{P}_0$) are needed, which are usually set to zero.

$\boldsymbol{Q}$ and $\boldsymbol{R}$ are the covariances of process noise, and measurement noise, respectively, and for simplicity, they are assumed as $\boldsymbol{Q} = [1, 0; 0, 1]$ and $R = 1$.

It should be noted that the input vector $\boldsymbol{u}$ is composed of the inverter output voltage and the load current. Evidently, the inverter output voltage can be replaced by the controller output to the PWM block, and therefore no measurement is needed. However, the load current which is also necessary for the protection purposes is measured directly.

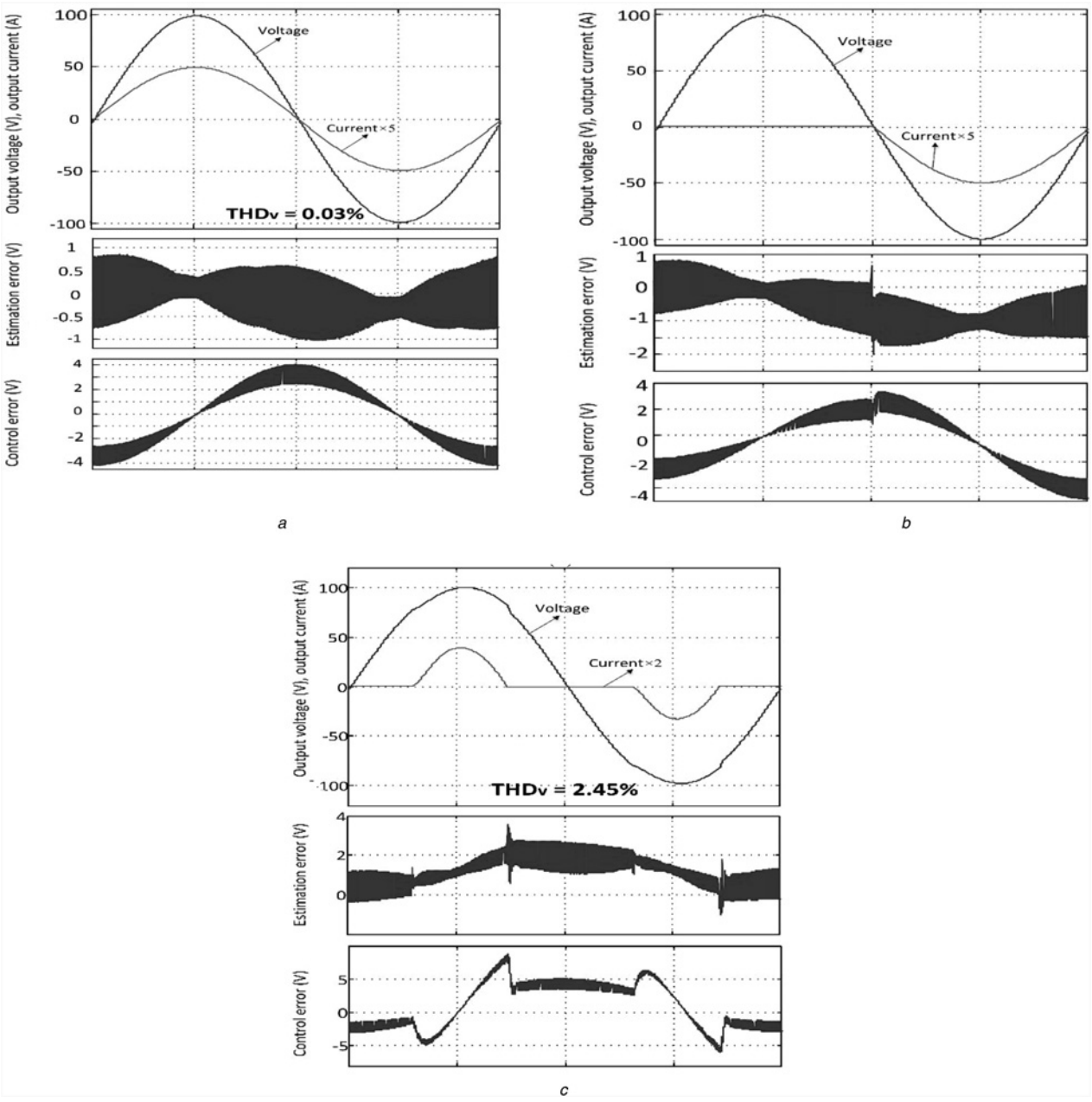

Fig. 7 *Measured output voltage, current and errors*

a Under the nominal linear load
b Transient from no load to full load
c Under a highly non-linear load

IET Power Electron., 2015, Vol. 8, Iss. 9, pp. 1817–1824

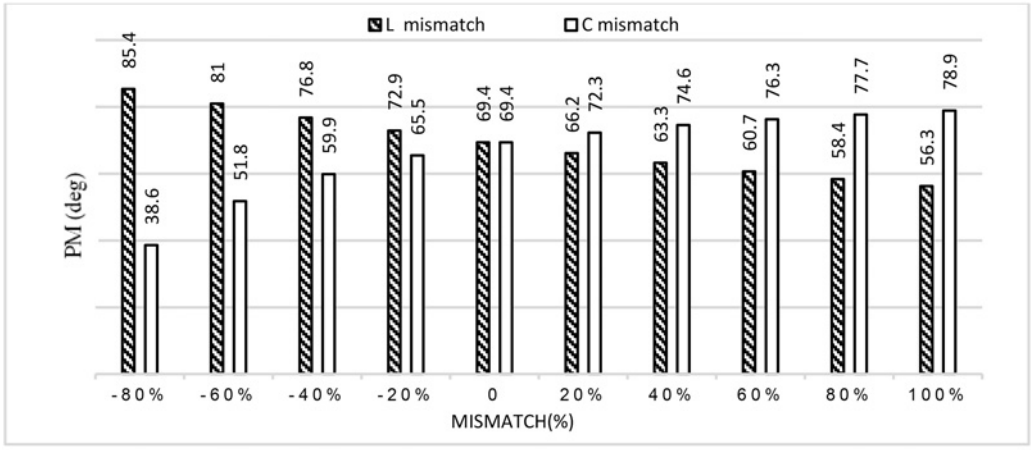

a

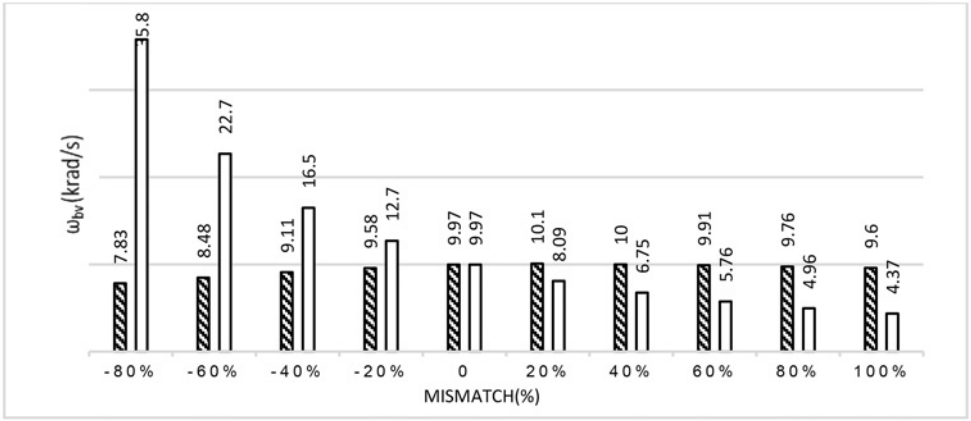

b

Fig. 8 *Effect of L and C mismatches (in per cent) on*
a PM
b Closed-loop control bandwidth

5 Performance evaluation

5.1 Stability margin in presence of digital control and estimation delays

The PM under the worst case was determined to be 69.4°. However, this value for PM cannot be achieved in practice, because of some practical effects, such as control and PWM delays, and dynamics of the estimator. Indeed, digital control systems impose an additional time delay in the control loop. This delay corresponds to the digital sampling, programme computation time and PWM register update and results in one PWM period delay in digital execution of the control algorithm [1]. Besides, the delay of estimator must be considered. The linear Kalman filter imposes one further sampling period delay. Therefore the overall effect of digital implementation and estimation dynamics can be simplified as a two sampling period delay. In this paper, each delay decreases the PM by about 14°. Therefore the new PM is about 41° and still adequate to ensure the system stability and avoid the oscillatory response.

5.2 Simulations

To verify the performance of the proposed control method, the single-phase UPS inverter is simulated in MATLAB/SIMULINK. Simulations are done under linear and non-linear loads in steady and transient states.

Fig. 7*a* shows the measured output voltage, measured output current and errors of estimation and control for the nominal linear load. The output voltage is highly sinusoidal with the total harmonic distortion (THD) of 0.03%. The estimation error is lower than 1%, which translates to an excellent estimation accuracy. The tracking error of the multi-loop control with simple proportional controllers and a feedforward of the reference voltage is limited to 4%.

Fig. 7*b* presents the transient performance in response to a no load to full load transition. The transient vanishes rapidly and both estimation and control errors remain almost unchanged during the load change. In fact, this excellent transient performance owes to the proper selection of the feedback quantity in the inner loop, because the capacitor current changes instantaneously with the load current change.

Moreover, the performance of the proposed control method is evaluated under a highly non-linear load and the results are shown in Fig. 7*c*. The non-linear load, designed according to IEC 62040-3 standard (Annex E), consists of a 1 Ω resistor in series with a diode rectifier bridge feeding a 6800 μF capacitor in parallel with a 20 Ω resistor. One can see in Fig. 7*c* that while the load current is highly distorted, with a THD of about 81% and a crest factor of about 3:1, the voltage waveform remains sinusoidal (THD = 2.45%). Moreover even in this strict condition, the estimated waveform tracks the actual one perfectly.

It should be noted that in practice, the parameters of the LC filter may not be exactly known or may vary depending on the operating conditions and ageing. The performance of the control system, without the estimator, in terms of the PM and the control bandwidth, considering mismatches in the L and C values, is investigated, and the results are summarised in Fig. 8. Fig. 8*a*

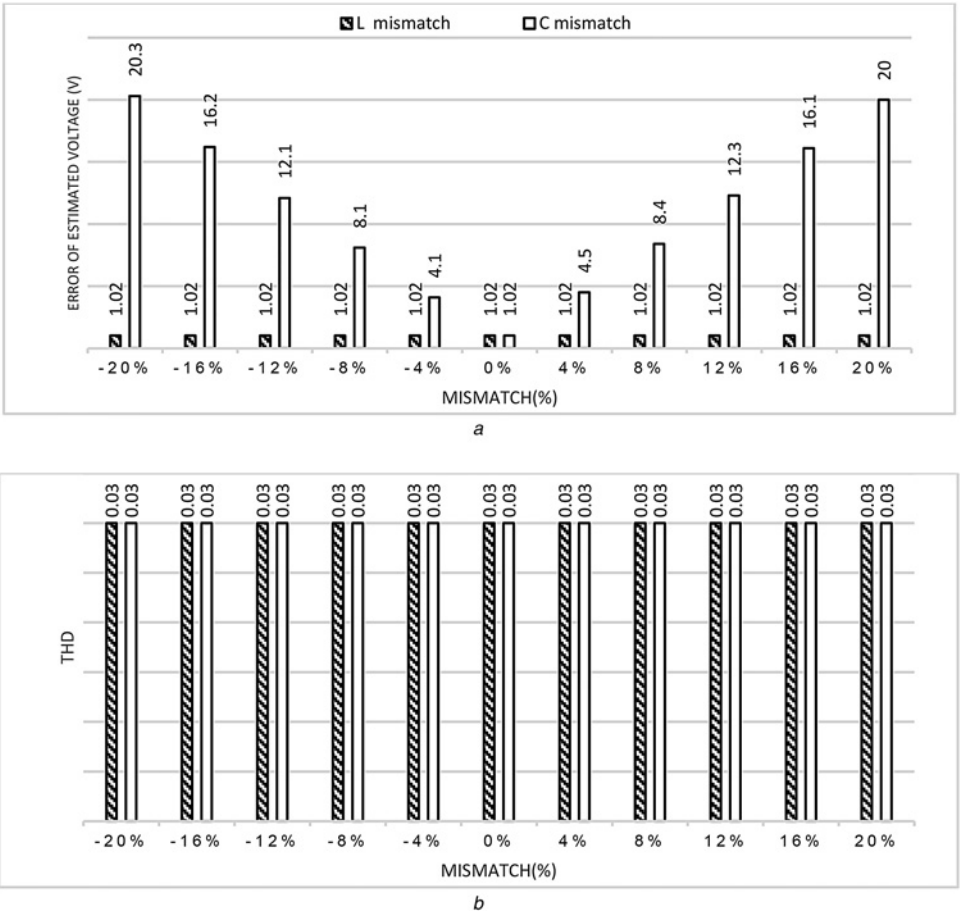

Fig. 9 *Effect of L and C mismatches (in per cent) on*

a Error of estimation
b THD of output voltage

shows that L and C uncertainties lead to PM variations; however, for a wide range of mismatches the PM is still adequate. Moreover, Fig. 8*b* shows that the ω_{bv} mainly remains unchanged with inductance mismatches; however, the capacitance uncertainties lead to large bandwidth variations, especially if the capacitor value is underestimated, then a remarkable increase in the voltage loop bandwidth is expected. This may cause the system response to be highly oscillatory or even unstable.

The performance of the estimator also is investigated, and the results are plotted in Fig. 9. Obviously, mismatches in the L and C values have no impact on the THD of the output voltage. Moreover, voltage estimator acts properly with inductance mismatches, but the capacitance uncertainties have high impact on the operation of the voltage estimator. This impact is caused by state-space equations in the Kalman filter algorithm, where the C value plays a significant role in these equations.

5.3 Experiments

A digitally controlled single-phase UPS is built to verify the conclusions drawn by the simulation studies. The experimental platform consists of a DC-link, which is fed from a three-phase diode-bridge rectifier, a full-bridge insulated gate bipolar transistor intelligent power module, an output LC filter, measurement circuits and gate drives.

The control and estimation algorithms are implemented with a TMS320F28335 32 bit floating-point digital signal controller from Texas Instruments.

The experimental system parameters are the same as the simulations.

In the first study, the steady-state behaviour of the proposed controller under the nominal resistive load is investigated and the results are shown in Fig. 10*a*, where the load voltage and the load current, as well as the estimation error are depicted. The output voltage is sinusoidal with a very low distortion and the performance of the estimator is excellent.

The transient behaviour of the system in response to a load step jump from no load to the nominal load is shown in Fig. 10*b*. It can be seen that the output voltage is not affected by the change in the load and the current regulator dynamic is very fast.

Finally and as a worst-case operation, a highly non-linear load similar to the simulated one connected to the UPS output and the results are shown in Fig. 10*c*. Despite the highly distorted load current, the load voltage is still sinusoidal (THD = 7.3%) and the estimation accuracy does not decrease compared with the linear loading condition. It should be noted that according to the IEC 62040-3 standard (Annex E), for this type of loading condition, the voltage THD is required to be <8%.

6 Conclusion

In this paper, a simple voltage sensorless multi-loop control method is proposed for the single-phase UPS inverter and the parameters are designed step-by-step based on the decided bandwidths for the control loops. The suggested control scheme uses two variables as feedback signals, which regulates them with simple proportional controllers instead of PI/PR controllers. For this purpose, the capacitor current is obtained indirectly from the measured converter and load currents, which are also necessary for the protection purposes and the load voltage is estimated by a simple

IET Power Electron., 2015, Vol. 8, Iss. 9, pp. 1817–1824

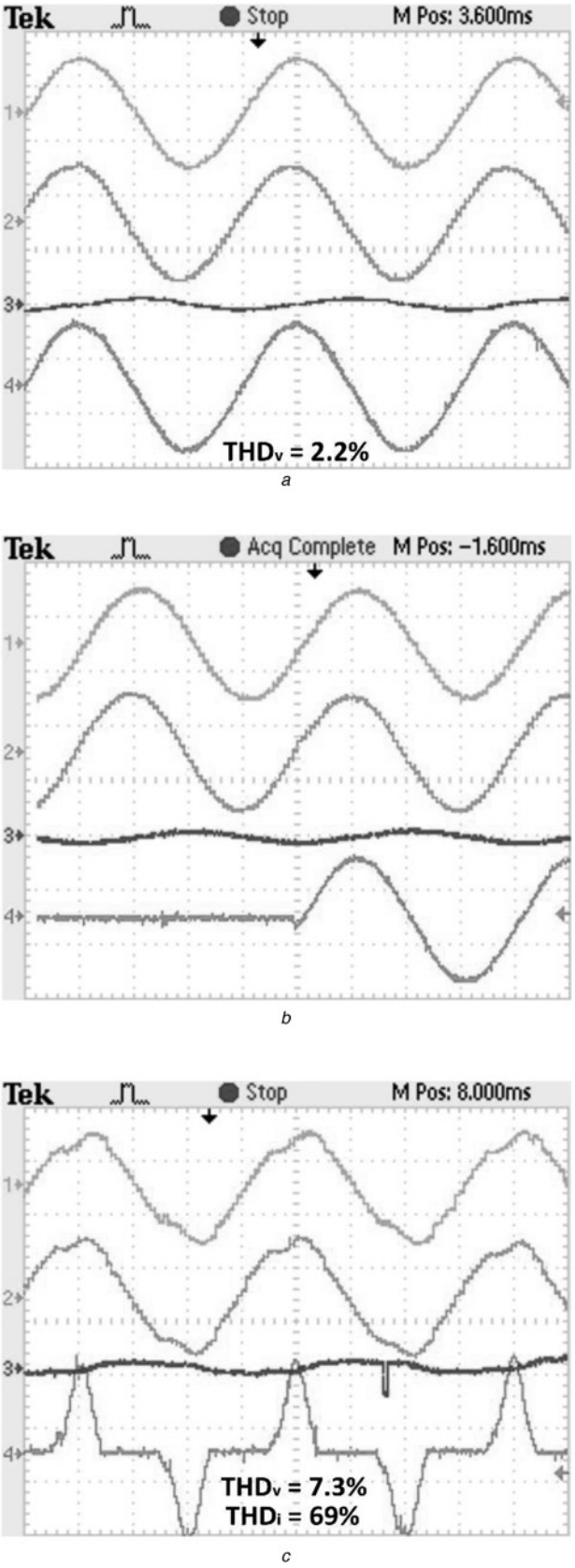

Fig. 10 *Experimental results*

a Steady-state waveforms for nominal resistive load ($R = 10\ \Omega$)
b Transient waveforms in response to no load to nominal resistive load step change
c Steady-state waveforms for a highly non-linear load
CH1: measured load voltage (100 V/div)
CH2: estimated load voltage (100 V/div)
CH3: voltage estimation error (100 V/div)
CH4: measured load current (8 A/div)

estimation algorithm based on the digital Kalman filter algorithm. The proposed controller does not need any reference frame transformation or integration/derivation of measured quantities. The excellent performance of the proposed control method is confirmed through extensive simulations and implementing it with a laboratory prototype.

7 References

1 Monfared, M., Golestan, S., Guerrero, J.M.: 'Analysis, design, and experimental verification of a synchronous reference frame voltage control for single-phase inverters', *IEEE Trans. Ind. Electron.*, 2014, **61**, (1), pp. 258–269
2 Kukrer, O., Komurcugil, H., Bayindir, N.S.: 'Control strategy for single-phase UPS inverters', *IEE Proc. Electron. Power Appl.*, 2003, **150**, (6), pp. 743–746
3 Mattavelli, P.: 'An improved deadbeat control for UPS using disturbance observers', *IEEE Trans. Ind. Electron.*, 2005, **52**, (1), pp. 206–212
4 Heng, D., Oruganti, R., Srinivasan, D.: 'A simple control method for high-performance UPS inverters through output-impedance reduction', *IEEE Trans. Ind. Electron.*, 2008, **55**, (2), pp. 888–898
5 Xu, S., Wang, J., Xu, J.: 'A current decoupling parallel control strategy of single-loop inverter with voltage and current dual closed-loop feedback', *IEEE Trans. Ind. Electron.*, 2013, **60**, (4), pp. 1306–1313
6 Abdel-rahim, N.M., Quaicoe, J.E.: 'Analysis and design of a multiple feedback loop control strategy for single-phase voltage-source UPS inverters', *IEEE Trans. Power Electron.*, 1996, **11**, (4), pp. 532–541
7 Ahmed, K.H., Massoud, A.M., Finney, S.J., Williams, B.W.: 'Autonomous adaptive sensorless controller of inverter-based islanded-distributed generation system', *IET Power Electron.*, 2009, **2**, (3), pp. 256–266
8 Zhang, K., Kang, Y., Xiong, J., Chen, J.: 'Direct repetitive control of SPWM inverter for UPS purpose', *IEEE Trans. Power Electron.*, 2003, **18**, (3), pp. 784–792
9 Yang, Y., Zhou, K., Lu, W.: 'Robust repetitive control scheme for three-phase constant-voltage-constant-frequency pulse-width modulated inverters', *IET Power Electron.*, 2012, **5**, (6), pp. 669–677
10 Ortega, R., Garcera, G., Figueres, E., Caranza, O., Trujillo, C.L.: 'Design and application of a two degrees of freedom control with a repetitive controller in a single phase inverter'. Proc. IEEE ISIE, 2011, pp. 1441–1446
11 Chen, S., Lai, Y.M., Tan, S.C., Tse, C.K.: 'Analysis and design of repetitive controller for harmonic elimination in PWM voltage source inverter systems', *IET Power Electron.*, 2008, **1**, (4), pp. 497–506
12 Jiang, S., Cao, D., Li, Y., Liu, J., Peng, F.Z.: 'Low-THD, fast-transient, and cost-effective synchronous-frame repetitive controller for three-phase UPS inverters', *IEEE Trans. Power Electron.*, 2012, **27**, (6), pp. 2994–3005
13 Komurcugil, H.: 'Rotating-sliding-line-based sliding-mode control for single-phase UPS inverters', *IEEE Trans. Ind. Electron.*, 2012, **59**, (10), pp. 3719–3726
14 Kukrer, O., Komurcugil, H., Doganalp, A.: 'A three-level hysteresis function approach to the sliding-mode control of single-phase UPS inverters', *IEEE Trans. Ind. Electron.*, 2009, **56**, (9), pp. 3477–3486
15 Tai, T.L., Chen, J.S.: 'UPS inverter design using discrete-time sliding-mode control scheme', *IEEE Trans. Ind. Electron.*, 2002, **49**, (1), pp. 67–75
16 Chen, S., Lai, Y.M., Tan, S.C., Tse, C.K.: 'Fast response low harmonic distortion control scheme for voltage source inverters', *IET Power Electron.*, 2009, **2**, (5), pp. 574–584
17 Mohamed, Y.A-R.I., El-saadany, E.F., El-shatshat, R.A.: 'Natural adaptive observers-based estimation unit for robust grid-voltage sensorless control characteristics in inverter-based DG units'. IEEE Power Engineering Society General Meeting, 2007, pp. 1–8
18 Cortes, P., Ortiz, G., Yuz, J.I., Rodriguez, J., Vazquez, S., Franquelo, L.G.: 'Model predictive control of an inverter with output LC filter for UPS application', *IEEE Trans. Ind. Electron.*, 2009, **56**, (6), pp. 1857–1883
19 Deng, H., Oruganti, R., Srinivasan, D.: 'Adaptive digital control for UPS inverter application with compensation of time delay'. Proc. IEEE Applied Power Electronics Conf., 2004, vol. 1, pp. 450–455
20 Gholami-Khesht, H., Monfared, M.: 'Novel grid voltage estimation by means of the Newton–Raphson optimization for three-phase grid connected voltage source converters', *IET Power Electron.*, 2014, **7**, (12), pp. 2945–2953
21 Ahmed, K.H., Massoud, A.M., Finney, S.J., Williams, B.W.: 'Sensorless current control of three-phase inverter-based distribution generation', *IEEE Trans. Power Deliv.*, 2009, **24**, (2), pp. 919–929
22 Loh, P.C., Newman, M.J., Zmood, D.N., Holmes, D.G.: 'A comparative analysis of multiloop voltage regulation strategies for single and three-phase UPS systems', *IEEE Trans. Power Electron.*, 2003, **18**, (5), pp. 1176–1185
23 Ahmed, K.H., Massoud, A.M., Finney, S.J., Williams, B.W.: 'A modified stationary reference frame-based predictive current control with zero steady-state error for LCL coupled inverter-based distributed generation systems', *IEEE Trans. Ind. Electron.*, 2011, **58**, (4), pp. 1359–1370
24 Vandoorn, T.L., Ionescu, C.M., De Kooking, J.D.M., De Keyser, R., Vandevelde, L.: 'Theoretical analysis and experimental validation of single-phase direct vs. cascade voltage control in islanded microgrids', *IEEE Trans. Ind. Electron.*, 2013, **60**, (2), pp. 789–798
25 Lim, J.S., Park, C., Han, J., Lee, Y.I.: 'Robust tracking control of a three-phase DC–AC inverter for UPS applications', *IEEE Trans. Ind. Electron.*, 2014, **59**, (1), pp. 4142–4151

26 Zou, Z., Wang, Z., Cheng, M.: 'Modeling, analysis, and design of multifunction grid-interfaced inverters with output LCL filter', *IEEE Trans. Power Electron.*, 2014, **29**, (7), pp. 3830–3839
27 Ryan, M.J., Brumsickle, W.E., Lorenz, R.D.: 'Control topology option for single-phase UPS inverters', *IEEE Trans. Ind. Appl.*, 1997, **33**, (2), pp. 493–501
28 Wai, R.J., Lin, C.Y., Wu, W.C., Huang, H.N.: 'Design of backstepping control for high-performance inverter with stand-alone and grid-connected power-supply modes', *IET Power Electron.*, 2013, **6**, (4), pp. 752–762
29 Hasanzadeh, A., Edrington, C.S., Maghsoudlou, B., Fleming, F., Mokhtari, H.: 'Multi-loop linear resonant voltage source inverter controller design for distorted loads using the linear quadratic regulator method', *IET Power Electron.*, 2012, **5**, (6), pp. 841–851
30 Simon, D.: 'Kalman filtering with state constraints: a survey of linear and nonlinear algorithms', *IET Power Electron.*, 2010, **4**, (8), pp. 1303–1318
31 Welch, G., Bishop, G.: 'An introduction to the Kalman filter'. Technical Report, TR 95-041, Department of Computer Science, University of North Carolina at Chapel Hill, 2004